ELSEVIER

Contents lists available at ScienceDirect

Geochimica et Cosmochimica Acta

journal homepage: www.elsevier.com/locate/gca





Anomalous ²³⁴U/²³⁸U isotopic composition in Southern Ocean sediments

N.A. Redmond ^{a,*}, C.T. Hayes ^a, S.K. Glasscock ^a, E. Rohde ^a, R.F. Anderson ^b, D. McGee ^c

- ^a University of Southern Mississippi, School of Ocean Science and Engineering, Stennis Space Center, MS, United States
- ^b Lamont-Doherty Earth Observatory of Columbia University, Palisades, NY, United States
- c Massachusetts Institute of Technology, Department of Earth Atmospheric and Planetary Sciences, Cambridge, MA, United States

ARTICLE INFO

Associate editor: Noah J. Planavsky

Keywords: Trace elements Deep sea diagenesis Sediment geochemistry Paleoredox Uranium

ABSTRACT

Uranium is a redox-sensitive trace element that under certain sedimentary conditions will reflect changes in past biological productivity and/or deep ocean ventilation. Applications for the isotopic composition of U $(^{234}\text{U};^{238}\text{U}$ activity ratio, δ^{234} U or the per mil deviation from secular equilibrium) as a paleoceanographic proxy, however, remain largely unexplored in pelagic sediments. We present $\delta^{234}U$ of bulk U for a 504-kyr record of South Atlantic core ODP 1094, a record that has exhibited sensitivity to bottom water formation with minimal ²³⁸U remobilization due to changes in redox condition. Sedimentary $\delta^{234}U$ at time of burial was modeled given authigenic and detrital sources, where it was found that $\delta^{234}U$ has a reoccurring pattern of anomalous behavior around deglacial transitions. In many cases, the anomalous δ^{234} U compositions in sediment exceeded seawater, which is not consistent with its expected sources. A mass balance of ²³⁴U across these anomalous sections showed that vertical rearrangement of 234 U can explain anomalous sedimentary δ^{234} U during Marine Isotope Stage (MIS) 7/8 and 11/12 transitions, as well as partially during MIS 5/6 and MIS 9/10. The distribution of these anomalies is likely consistent with the idea that deglacial spikes in aU, resulting from periods of high organic carbon delivery and thereby strong reduction in the sediments, act as a persistent sink of ²³⁴U alpha-recoiled from vertically adjacent sediment layers after burial. While this mechanism explains the negative $\delta^{234}U$ anomalies, there is a large subset of positive $\delta^{234}U$ anomalies that cannot be explained by vertical diffusion of ^{234}U in pore waters alone. This excess 234 U points to an extremely high δ^{234} U source to seawater during deglaciation or additional diagenetic effects such as diffusion from lateral heterogeneity in the redox state of sediment at depth. We find that δ^{234} U of pelagic sediment may be useful to identify fine-scale pore water migration of alpha-recoil products

1. Introduction

The Southern Ocean acts as a hub for thermohaline circulation and is an important driver of global heat, nutrient, and carbon cycles. One of its more salient elements is the formation of Antarctic Bottom Water, which is a control on deep ocean circulation and glacial carbon transport. During glacial periods, there is reduced atmospheric carbon dioxide (Delmas et al., 1980). This carbon must ultimately have been stored in the deep ocean during these periods as this is the only mechanism where the reservoirs equilibrate on needed time scales (Broecker, 1982), although the mechanisms for this process are still being debated (Sigman et al., 2010). Regardless, any increase in the carbon storage capacity of the biological pump, which ultimately decrease atmospheric CO₂ concentrations, also lowers the inventory of deep sea dissolved oxygen proportional to the Redfield ratio of respiration (Broecker, 1982; Sigman

et al., 2010). This relationship allows for past ocean carbon storage to be qualitatively constrained using deep sea dissolved oxygen budgets (Anderson et al., 2019; Francois et al., 1993). One method to assess oxygen delivery to the deep sea by bottom water ventilation, when combined with proxies for organic matter flux, is the use of redox-sensitive trace metals in sediment (Francois et al., 1997).

One such redox tracer is U, which is soluble and well-mixed throughout the world's oxygenated oceans; however, U becomes insoluble in suboxic pore waters (Ku et al., 1997). In an oxygenated water column, U forms soluble uranyl-carbonate species, however in anoxic or suboxic conditions, reduces from its hexavalent state to an insoluble tetravalent state. Its residence time in seawater far exceeds the time scale of global ocean mixing and individual glacial-interglacial cycles, leading to the assumption that U chemistry is relatively unchanged over these time scales (Esat and Yokoyama, 2006). Authigenic uranium (aU),

E-mail address: Neil.Redmond@usm.edu (N.A. Redmond).

^{*} Corresponding author.

which is formed by *in situ* precipitation in oxygen depleted pore waters, has been used as a proxy for changes in circulation/ventilation (Francois et al., 1993; Hayes et al., 2014) and organic carbon delivery (Jaccard et al., 2013). The other major component of U flux to the sediments is detrital U, supplied via continental sources including rivers, aeolian dust deposition, or ice rafted debris. Because of its redox sensitivity, records of U are potentially prone to post-depositional alteration, such as "burndown", which can complicate the use of U as redox paleoproxies (Wilson et al., 1986). This study explores bulk sedimentary U isotope ratios as a diagnostic tool for the diagenesis of U after burial.

$$\delta^{234}U = \left(\left(\frac{^{234}U}{^{238}U_{meas}} / \frac{^{234}U}{^{238}U_{eq}} \right) - 1 \right) * 1000$$
 (1)

where $\delta^{234}U$ is the isotopic composition of U as a per mil (%) deviation from secular equilibrium. $(^{234}U/^{238}U)_{meas}$ is the measured activity ratio and $(^{234}U/^{238}U)_{eq}$ is the activity ratio of U isotopes at secular equilibrium.

Both aU and detrital U have unique U isotopic compositions stemming from systematic fractionation during the U cycle. Variations in δ^{234} U from secular equilibrium occur from alpha-recoil, where the alpha-decay of ²³⁸U ejects its daughter isotope ²³⁴Th out of the mineral lattice entirely or into a damaged lattice site. Subsequently ²³⁴Th (halflife 24.1 days, Knight and Macklin, 1948) and its daughter ^{234m}Pa (halflife 1.17 min, Firestone et al., 1998) beta-decay into the longer-lived ²³⁴U (half-life 245,620 yrs, Cheng et al., 2013). Alpha-recoil thereby gives ²³⁴U a tendency to leave its mineral host by a process independent of its chemistry (Henderson and Anderson, 2003). At macroscales, this effect leads to preferential loss of ²³⁴U in terrestrial rock, creating a flux of ²³⁴U to marine systems from terrestrial riverine discharge and a flux from marine sediment pore-waters also enriched by alpha-recoil (Henderson, 2002; Ku, 1965). In marine sediment, alpha-recoil creates a pool of ²³⁴U that is reactive and prone to remobilization (Gourgiotis et al., 2011; Maher et al., 2004), which may be preferentially mobilized during sedimentary diagenesis. These inputs of ²³⁴U from alpha-recoil keep δ²³⁴U seawater above secular equilibrium with a modern global average of 146.8 \pm 0.1% (Andersen et al., 2010). There is evidence to show this global seawater value fluctuates over glacial-interglacial cycles, as coral records support changes as high as $\sim \pm 15\%$ (Esat and Yokoyama, 2006; Yokoyama et al., 2001). However, more recent assessments have suggested the Last Glacial Maximum seawater δ^{234} U may have been closer to 5-7% lower than modern seawater composition (Chen et al., 2016; Chutcharavan et al., 2018) and relatively constant throughout the late Quaternary (Henderson, 2002; Robinson et al., 2004). In some environments, such as during the anoxic formation of shallow carbonates, the change in form from seawater U(VI) to sedimentary U(IV) can induce a $\delta^{234} U$ mass fractionation of ${\sim}0.8{\text{--}}1.6\%$ heavier than expected (Romaniello et al., 2013). Authigenic U precipitation in the pelagic ocean should, at least initially, reflect the δ^{234} U seawater composition. Detrital sediments are expected to have $\delta^{234}U$ close to secular equilibrium (0%) due to radioactive decay, however, due to loss of ²³⁴U from alpha-recoil, can be slightly negative (Thomas et al., 2007). The exact δ^{234} U of detrital materials can vary as the amount of 234 U lost from alpha-recoil is a function of 1. Sediment age since formation by mechanical erosion and 2. Grain size (DePaolo et al., 2006, 2012). Given the half-life of 234 U (\sim 254 ka), a steady state between 234 U and 238 U is reached after 1 Ma that depends only on grain size (DePaolo et al., 2006, 2012). For larger grains ($>65 \mu m$), this steady state is roughly the same as secular equilibrium (0%), but for smaller grain sizes, the fractional loss of ²³⁴U can be between a few percent and ~50%, with the expectation that the $\delta^{234} U$ of fine silts sediment (~10 $\mu m)$ is ~240% (Bourne et al., 2012; DePaolo et al., 2006, 2012).

2. Materials and methods

2.1. ODP 1094

ODP 1094 (Leg 177, 53.18035° S, 5.130333° E, 2807 m water depth, Fig. 1) is an Atlantic-sector Southern Ocean core situated between the Antarctic Polar Front to the north and the southern boundary of the Antarctic Circumpolar Current to the south. This location is close to the Weddell Sea, a known site for the formation of Antarctic Bottom Water, and the core site is bathed by Circumpolar Deep Water (Shipboard Scientific Party, 1999a). ODP 1094 primarily consists of Pleistocene age diatomaceous ooze (60-80% biogenic opal; Shipboard Scientific Party, 1999a) during interglacial sections, with punctuated increases in volcaniclastic particles and quartz derived from ice rafted debris (IRD) present during glacial periods (Kanfoush et al., 2002; Nielsen et al., 2007), and a relative lack of calcium carbonate (<1%), except during deglacial intervals where CaCO3 reaches at most 10% (Jaccard et al., 2013). Present day redox conditions of bottom water at this location are generally well oxygenated (average dissolved O2 concentration of ~200-230 µM) due to influx of recently ventilated subsurface water masses (Jaccard et al., 2016). Previous efforts have reconstructed ODP 1094's paleoredox conditions using aU over the past 150 ka (Hayes et al., 2014) and 500 ka (Glasscock et al., 2020); these studies ultimately showed that aU in this area is sensitive to redox changes in sediments from both increases in organic matter delivery and sluggish bottom water ventilation. Additional paleoredox constructions using aU, Mn, and Re have shown that ODP 1094 has experienced constantly sub-oxic conditions over the last 500 ka, which makes oxic remobilization of authigenic trace metals unlikely (Rohde et al., 2021).

ODP 1094's age model was constructed using paleomagnetic and biostratigraphic markers (Shipboard Scientific Party, 1999b) which have been further refined by tuning the oxygen isotopes of benthic foraminifera to the LR04 global benthic stack (Hasenfratz et al., 2019; Lisiecki and Raymo, 2005) (Fig. 2). The greatest certainty in the age model is during deglacial transitions, having 3–4 tie points in <10 ky, however this age model is less confined during other periods. Given the average sedimentation rate, an age model uncertainty of $\sim\!5.5$ ky can create an offset of 1 m in the U record with other proxies. For this study, the section of ODP 1094 analyzed was between 0.57 and 76.29 m composite depth (corresponding to ages of $\sim\!1$ to 504 ka), and new results were combined with the bulk U data presented in Hayes et al., 2014 and Glasscock et al., 2020. The average sedimentation rate for this section was $\sim\!17$ cm/ka, with sampling rate intervals of 10 cm to create sub millennial resolution.

2.2. Isotopic measurements

U isotope data covering the period 0 to 504 ka were produced in three laboratories (at the Lamont-Doherty Earth Observatory Data, the Massachusetts Institution of Technology, and the University of Southern Mississippi, respectively). All three labs used similar methods for strong acid digestions and total dissolution of the sediments, and preconcentration with iron (oxy)hydroxide co-precipitation, followed by anion exchange chromatography, to analyze uranium isotopes using isotope dilution with 236 U (Glasscock et al., 2020; Hayes et al., 2014, 2017). The main difference in sediment digestion techniques is that the Lamont lab used perchloric acid during digestions with HNO3, HCl and HF, while the MIT and USM labs did not use perchloric acid but still achieved total sediment dissolution using a combination of HNO3, H2O2, HCl and HF.

Data for ²³⁴U activities from the 0 to 157 ka section (144 samples at roughly millennial resolution) were produced initially at the Lamont-Doherty Earth Observatory in 2010–2012. The Lamont data were analyzed using a single-collector, VG Axiom inductively-coupled plasma mass spectrometer (ICP-MS). Corrections for tailing of the ²³⁵U peak onto measured ²³⁴U count rates were made using the geometric mean of

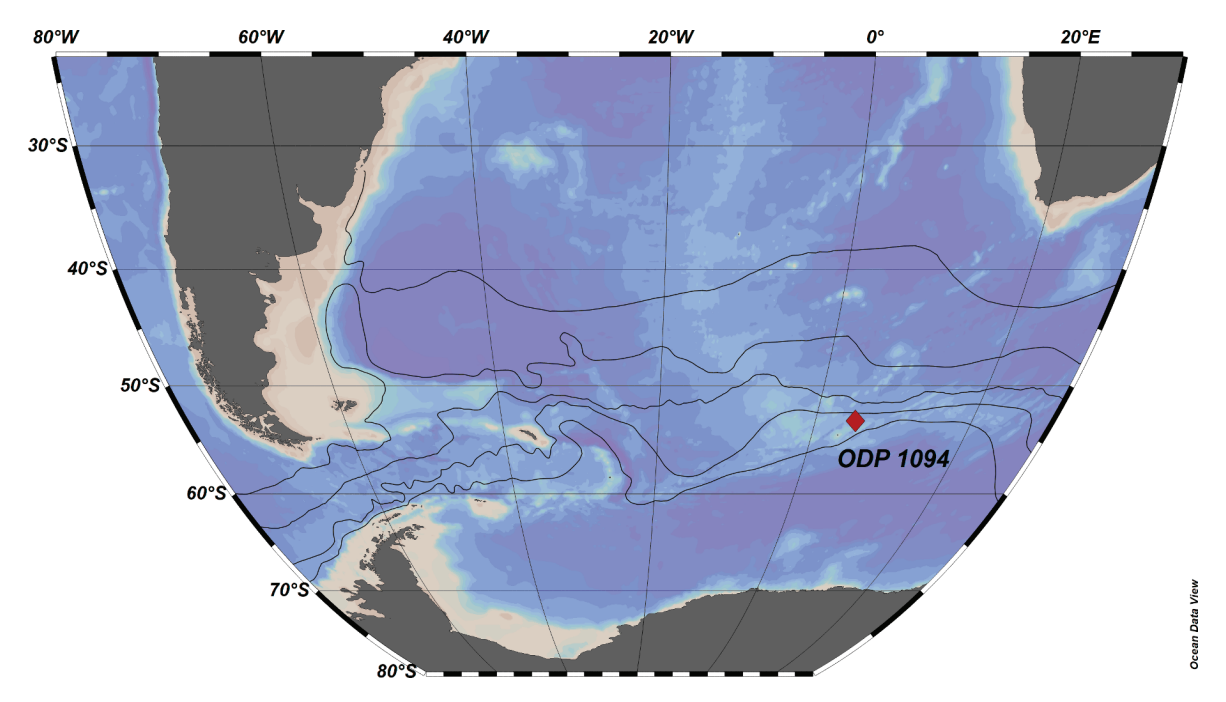


Fig. 1. ODP 1094 (53.18035° S, 5.130333° E, 2807 m) is in the center of the ice-free Antarctic Zone bounded by the Polar Front to the north and the Southern Antarctic Circumpolar Current boundary to the south (Shipboard Scientific Party, 1999b). Black lines show Southern Ocean fronts as defined in (Orsi et al., 1995); (North to South) Subtropical Front, Sub-Antarctic Front, Antarctic Polar Front, and the southern boundary of the Antarctic Circumpolar Current.

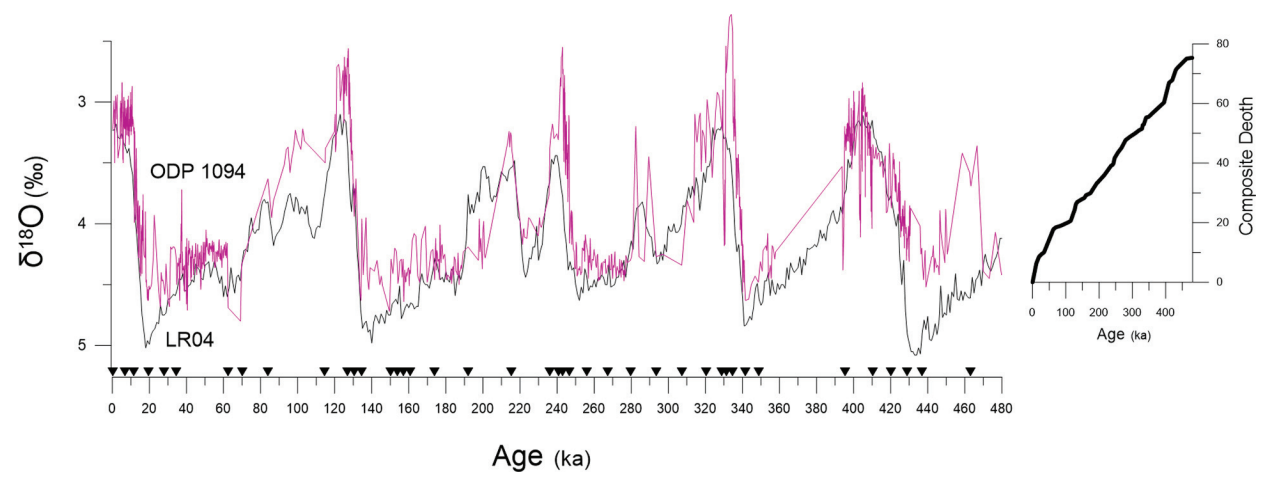


Fig. 2. Global stack of benthic δ^{18} O (black) from (Lisiecki and Raymo, 2005) (LR04) shows changes in global glaciation. The benthic δ^{18} O for ODP 1094 (pink) from Hasenfratz et al., 2019 is tuned according to the LR04 stack (tie points shown with black triangles). The inset figure shows the age to depth model used in Hasenfratz et al., 2019.

the count rates at mass-to-charge ratios 233.5 and 234.5. Corrections for instrumental mass bias were made by bracketing samples with standard solutions of SRM129 every 5–10 samples, and blank corrections on ^{238}U and ^{234}U were less than 0.2% of measured signals. The average precision on $\delta^{234}\text{U}$ values for samples and standards was 12‰. Duplicate digestions were analyzed (n = 7) and the $\delta^{234}\text{U}$ of duplicates agreed within an average of 27‰. The bulk U concentrations from this work were used in published studies (Hayes et al., 2013; Jaccard et al., 2013) for which only the ^{238}U activities were necessary, and the ^{234}U activities were not published at that time. As a point of historical context, in the Lamont data an anomaly of measured and decay corrected $\delta^{234}\text{U}$ was found of $\sim\!200\%$, higher than $\sim\!147\%$, the ratio in seawater, during Marine Isotope Stage (MIS) 5 (specifically around 127 ka), which will be described more fully in results. Because of the relatively large uncertainties in the Lamont $\delta^{234}\text{U}$ data, there was some question whether

these data were of high enough quality to merit further investigation. Therefore, we sought to confirm the anomalous finding using a higher precision multi-collector ICP-MS.

In 2014, a suite of 24 samples from throughout the 38 to 155 ka sections were analyzed at MIT on a Nu Plasma II multi-collector ICP-MS, capable of an improved average precision on samples and standards of 2‰. At MIT, every sample was bracketed with a standard solution of CRM-112a and ^{234}U was analyzed on the central ion multiplier, with ^{238}U being analyzed on a Faraday cup simultaneously. A peak jumping routine also had to be used to measure count rates at mass-to-charge ratios of 233.5 and 234.5 on the ion multiplier for a ^{234}U tail correction similar to that described above. MIT blank corrections were less than 0.1% on U isotopes. These data confirmed the large positive $\delta^{234}\text{U}$ anomaly around 127 ka (Fig. 3) and gave confidence that any further anomalies in $\delta^{234}\text{U}$ were likely resolvable using the lower precision

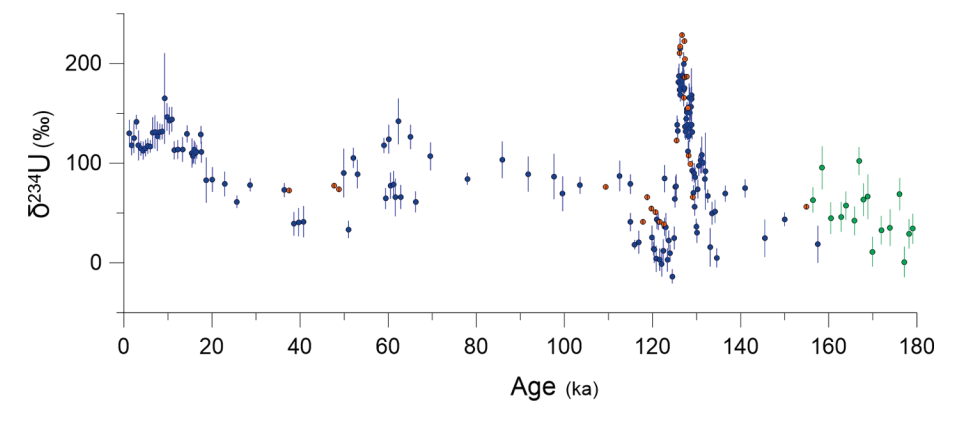


Fig. 3. Bulk observed δ²³⁴U (‰, per mil) in ODP 1094 as a function of sediment age illustrating the results from overlapping sections analyzed by three labs (blue – Lamont-Doherty Earth Observatory, orange – Massachusetts Institute of Technology, green – University of Southern Mississippi).

single collector, Element HR-ICP-MS at USM.

We now turn to provide more details on the procedures used to determine δ^{234} U at USM (Fig. 4) from 2017 to 2019 in sections of ODP-1094 covering 156 to 504 ka, (280 samples at roughly millennial resolution). Freeze-dried sediment samples of 50 mg were spiked with a known quantity (0.1 ng) of 236 U (Eckert & Ziegler Isotope Products) and

then dissolved in a series of digestions including HNO₃, $\rm H_2O_2$, HCl and HF, as described by Glasscock et al. (2020). Once fully dissolved, 2–3 mg of iron, as dissolved iron chloride, was added to the solution and pH was raised using drops of NH₄OH until an iron oxyhydroxide containing the U was precipitated. U was extracted via column chromatography on Dowex 1X8 resin. Count rates of 234 U, 235 U, and 236 U were measured on

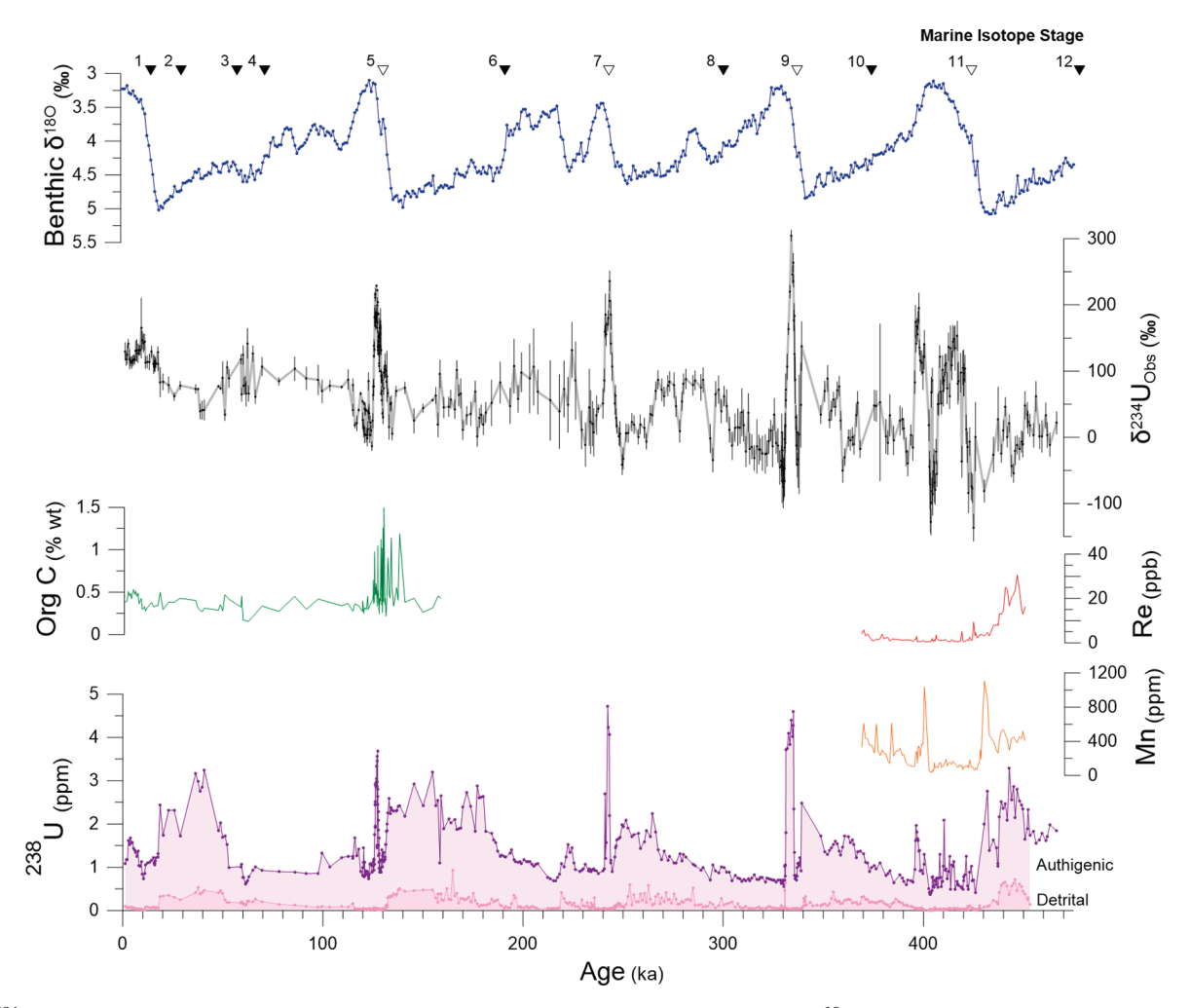


Fig. 4. δ^{234} U in ODP 1094 over the last 480 ka. Marine Isotope Stages (triangles) are defined by the benthic δ^{18} O record (blue, from Lisiecki and Raymo, 2005) and reflect changes in global ice volume. Observed bulk δ^{234} U (black) shows generally increased values during spikes in 238 U (purple) surrounding glacial terminations (marked as white triangles for MIS 5/6, 7/8, 9/10, and 11/12 transitions). Organic carbon (green) is shown from MIS 5/6 to present. Redox sensitive trace metals Re (red) and Mn (orange) are presented from MIS 10–12 from Rohde et al., 2021. Total sedimentary 238 U (purple) is divided into two fractions; aU (purple area) and detrital U (pink area) from Glasscock et al., 2020.

the Thermo Element HR-ICP-MS at USM. The ICP-MS analysis method was similar to that described for the Lamont lab above, using solutions of CRM-112a bracketing every 5–10 samples to correct for instrumental mass bias and making a tail correction based on count rates at mass-to-charge ratios 233.5 and 234.5. Decay-corrected δ^{234} U values were calculated based on measured 234 U/ 235 U ratios, assuming a seawater 238 U/ 235 U ratio of 137.83 (Andersen et al., 2016) and the following half-lives (234 U, $^{2.456}\times10^{5}$ yr; 238 U, 235 U here and avoiding the measurement of the most abundant isotope, 238 U, allowed measurement of a higher signal of 234 U. The subper mil level variation of 238 U/ 235 U in the ocean (Andersen et al., 2017) causes a negligible change in δ^{234} U calculated this way. The average precision of δ^{234} U for the USM data was 22‰. Blank corrections on U isotopes were less than 0.2% of measured signals. Duplicate (n = 37) and triplicate (n = 4) digestions were analyzed and the average standard deviation of replicate measurements was 26‰.

2.3. Model for predicting bulk $\delta^{234}U$

An endmember mixing model (Fig. 5, gray line) was made to predict $\delta^{234}U$ at depth using the following steps; 1. Calculation of aU and detrital U from $^{232}Th/IRD$ (Eqs. (2) and (3)), 2. Mixing of aU and detrital U fractions with known $\delta^{234}U$ (Eq. (4), and Fig. 5, blue and purple), and 3. Decay for comparison to modern observed data (Eq. (4)). The uncertainty for these predictions was propagated using the uncertainty of the lithogenic $^{238}U/^{232}Th$ mass ratio and uncertainty in the $\delta^{234}U$ of detrital U (Fig. 5, gray envelope).

The fraction of aU and detrital U were calculated as follows:

$$[aU] = [U_{bulk}^* (1 - F_{U,det})] \tag{2}$$

where [aU] is the concentration authigenic U in ppm ($\mu g/g$). U_{bulk} is the concentration of U in bulk sediment in ppm. $F_{U,det}$ is the fraction of total U that is detrital.

$$F_{U,det} = \frac{\left[^{232}Th\right] * \left(\text{lithogenic } \frac{^{238}U}{^{232}Th} \text{mass ratio}\right)}{U_{bulk}}$$
(3)

where $F_{U,det}$ is the fraction of total U that is detrital. [^{232}Th] is the

concentration of 232 Th in bulk sediment in ppm. The lithogenic 238 U/ 232 Th mass ratio is representative of terrigenous materials. U_{bulk} is the concentration of U in bulk sediment in ppm.

Given the assumption that the observed concentration of bulk sedimentary U (ppm) is a conservative mixing of authigenic and detrital fractions, determining one of these fractions allows for the calculation of each component's relative concentration (ppm) (Eq. (2)). The detrital fraction of bulk sedimentary U, F_{U,det}, can be estimated from measurements of ²³²Th (ppm) (Eq. (3)), an isotope assumed to be of entirely lithogenic origin, by using lithogenic ²³⁸U/²³²Th activity ratio representative for its ocean basin (Brewer et al., 1980; Henderson and Anderson, 2003). To account for potential variability of this site, a range of 0.4 to 0.7 was used (Henderson and Anderson, 2003). For these calculations, the activity ratio was converted to mass which yielded a lithogenic 238 U/ 232 Th mass ratio of 0.178 \pm 0.049. While 232 Th concentration can be used to calculate detrital material from its concentration of detrital material, this relationship is dependant on the ratio of volcanics to upper continental crust. Comparitively, the ratio of lithogenic ²³⁸U/²³²Th is relativley constant on a regional scale and can be used to calculate aU without assuming the volcanic to upper continental crust composition of the sediment. Measurements of ²³²Th were taken for two intervals: 0-155 ka and 370-450 ka. In these intervals, a strong correlation existed between ²³²Th concentrations and IRD (²³²Th (dpm/ g) = 0.0034 * IRD (grains/g) + 0.065, R = 0.79, n = 203, p < 0.00001, updated from Glasscock et al., 2020). For samples in which ²³²Th was not measured, ²³²Th concentrations were estimated from this relationship using IRD records from Kanfoush et al., 2002.

$$\delta^{234} U_{bulk,t} = ((1 - F_{\text{U,det}}) \delta^{234} U_{sw} + F_{U,det} \delta^{234} U_{det}) *e^{-\lambda_{234}t}$$
(4)

where $\delta^{234}U_{bulk,t}$ is the predicted U composition of bulk sediment U at core age t. $\delta^{234}U_{sw}$ is the U isotopic composition of seawater. $\delta^{234}U_{det}$ is the U isotopic composition of detrital sediments.

The expected isotopic composition of bulk U at sediment age (t) is given by a combination of each source's relative fraction and composition (both unitless), accounting for the decay of 234 U (e $^{-\lambda 234}$) for direct comparison with present day values (Figs. 5 and 6). The 8234 U of modern seawater used was 147% (Andersen et al., 2010). Although there is likely some error associated with the 8234 U of seawater over glacial

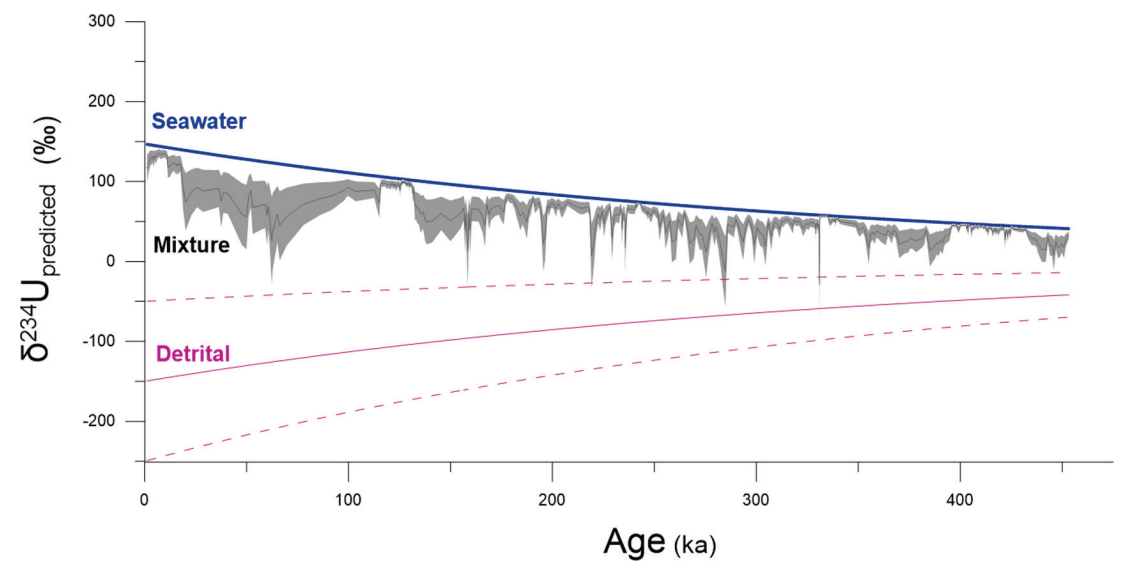


Fig. 5. Model of predicted bulk δ^{234} U given its sources at time of burial, accounting for each source's decay with age for comparison to modern measurements. The model (gray) is a function of sediment age given authigenic U (blue) and detrital U (purple) endmembers. The colored lines show age-decayed, pure endmember composition for aU (blue, decayed from $\sim 147\%$), and detrital U (purple, decayed from -150, dotted lines show uncertainty decayed from $\pm 100\%$). The predicted δ^{234} U (gray line) is created using Eqs. (2), (3) and (4), and uses the detrital U fraction calculated using a lithogenic mass ratio of 0.178, δ^{234} U of aU decayed from 147%, and δ^{234} U of detrital U decayed from -150%. The uncertainty of predicted δ^{234} U (gray envelope) is propagated from the uncertainty in determining the detrital fraction (Eq. (3), lithogenic δ^{238} U/ δ^{232} Th mass ratio δ^{234} U (and the uncertainty of detrital δ^{234} U (Eq. (4), δ^{234} U (Eq. (4), δ^{234} U).

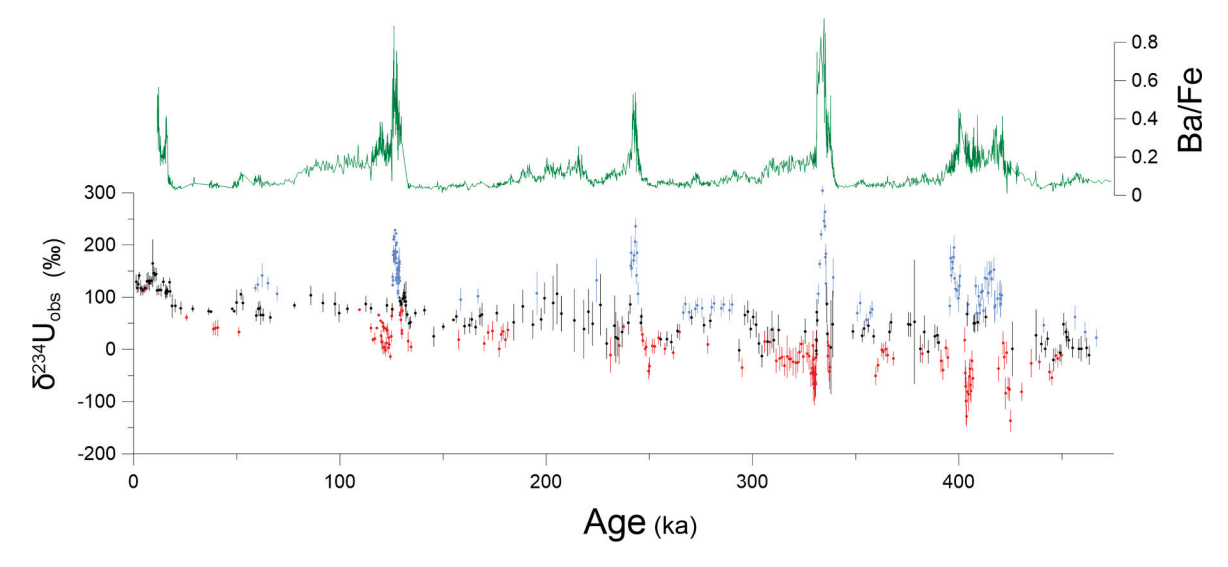


Fig. 6. Ba/Fe (green) shows the record of productivity at ODP 1094 (Jaccard et al., 2013), which illustrate periods of increased organic carbon flux. Observed bulk δ^{234} U is colored by its relationship to predicted bulk δ^{234} U. If the range of uncertainty of predicted δ^{234} U and the range of uncertainty of observed δ^{234} U intersect, data is considered within model expectations (black). Data were considered above (blue) or below (red) model expectations if the range of uncertainty of observed bulk δ^{234} U is greater than or less than predicted bulk δ^{234} U respectively.

cycles due to changes in physical weathering, a box model by (Henderson, 2002) has shown that δ^{234} U probably couldn't have changed more than 10% over 800,000 years, leading up to believe any error is relatively small. To account for the potential variability in δ^{234} U composition of detrital U, a range of -50 to -250% (-150 ± 100 %) was used in accordance with the model of (DePaolo et al., 2006) which accounts for potential grain size differences and age of detrital materials.

2.4. Mass balance

A mass balance was created by backtracking isotope data into a 234 U budget with the purpose of determining whether observed alterations of U isotopes can be explained by simple rearrangement, or migration, of 234 U. The mass of 234 U per sediment volume at each data point was integrated using simple trapezoids to estimate the total 234 U mass in each section (Eq. (5)). The same process was applied to the model of predicted δ^{234} U (Eq. (6)) and then the difference between these two represent the total quantified 234 U mass anomaly (Eq. (7)):

$$^{234}U_{obs} = \int_{-1}^{z^2} \rho_{sed} \frac{*[^{238}U]*(1 + (1000*\delta^{234}U_{obs}))*SA^{238}U}{SA^{234}U}$$
 (5)

$$^{234}U_{pred} = \int_{1}^{22} \rho_{sed} \frac{*[^{238}U]*(1 + (1000*\delta^{234}U_{mod}))*SA^{238}U}{SA^{238}U}$$
(6)

$$^{234}U_{anomaly} = ^{234}U_{obs} - ^{234}U_{nred}$$
 (7)

Total mass of predicted and observed ^{234}U (g/cm²) is a function of dry bulk density of sediment ($\rho_{sed},$ g/cm³), observed concentration of ^{238}U in sediment ($[^{238}\text{U}],$ g/cm²), and the specific activities of ^{238}U (SA ^{238}U , 1.24 \times 10 4 Bq/g, Jaffey et al., 1971) and ^{234}U (SA ^{234}U , 2.30 \times 10 8 Bq/g, Cheng et al., 2013), integrated over depths z1 and z2 (cm) with respect to core sections. For data points where the observed and predicted $\delta^{234}\text{U}$ agreed within uncertainties, the mass difference was integrated as zero. Sections where $^{234}\text{U}_{anomaly}$ is positive are designated as "excess" to show that they have gained ^{234}U since deposition whereas sections where $^{234}\text{U}_{anomaly}$ is negative are designated as "deficient" to show that they have lost ^{234}U since deposition. In some cases, the pattern of excesses and deficiencies represent potential diagenetic pathways as ^{234}U may move from deficiency to excess. This mass balance was done

for four specific intervals (Fig. 7), potentially representing diagenetic alteration at MIS 5/6, 7/8, 9/10, and 11/12, where observed bulk δ^{234} U was found to be greater than its seawater endmember. Additionally, this mass balance was conducted for our entire record of ODP 1094 as a means to look at larger scale sources and alterations. In future work, laboratory techniques to physically separate detrital and authigenic fractions (Martin et al., 2015) might help constrain our model's range associated with the detrital fraction and its isotopic value.

3. Results

3.1. Observed aU and δ^{234} U records

Authigenic U was the dominant form of U in ODP 1094, on average consisting of 90.5% of the bulk sediment fraction. ODP 1094 displays generally lower aU concentration during interglacial intervals and higher concentrations during glacial periods (Fig. 4). Among deglacial transitions, the aU behavior is not identical, although some features appear in multiple cycles. For the glacial terminations at MIS 5/6, 7/8, and 9/10, aU concentration drops precipitously at the start of deglaciation, and these drops are followed by peaks of aU concentration. These peaks of aU concentration fall sharply concurrent with the end of deglaciation as organic fluxes begin to fall. MIS 5/6 differs from this group in that it has an additional aU peak around 127 ka associated with a change in Antarctic Bottom Water formation (Hayes et al., 2014; Zhou and McManus, 2022). MIS 11/12 is similar, although these features are spread out more, which reflects the longer time scale of this termination. MIS 11/12 shares an initial drop in relative aU concentration at the start of the glacial termination, followed by a series of small concentration peaks which extend into the glacial period. The MIS 11 aU concentration peak at 395-401 ka is similar to that of 127 ka which is believed to be reflective of sluggish bottom water conditions (Glasscock et al., 2020). The most recent glacial termination (<20 ka) appears to show a small peak aU concentration.

There are some apparent similarities of the δ^{234} U record to aU concentrations, although they are not directly comparable. The most striking feature in this comparison is similar peaks in δ^{234} U and aU in the sections surrounding glacial terminations (Fig. 4). There was no significant correlation between δ^{234} U to aU throughout the whole record; however, there seems to be a general relationship near deglacial transitions. Generally, both aU and δ^{234} U seem to be enriched around

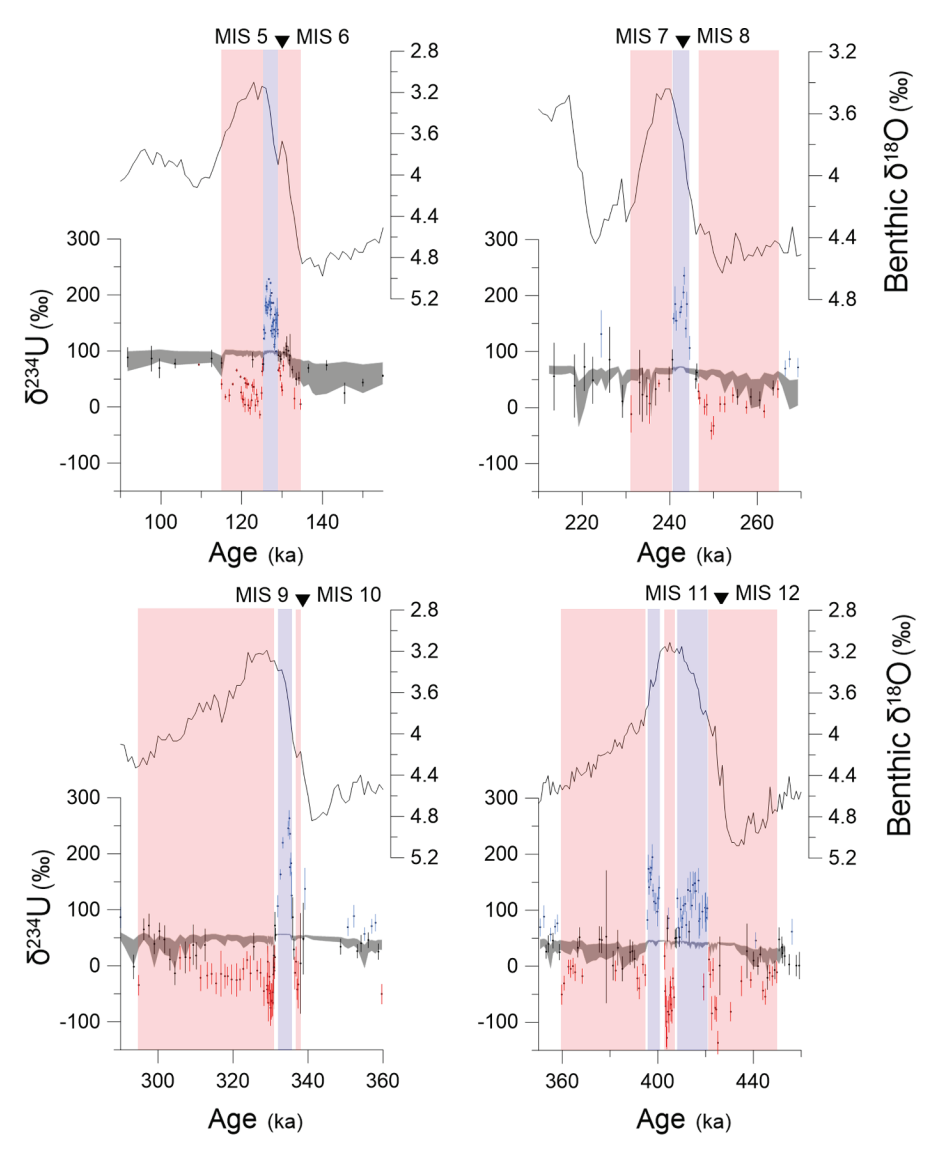


Fig. 7. Characterization of four δ^{234} U anomaly sections, MIS 5/6, 7/8, 9/10, and 11/12, used for mass balance. Benthic δ^{18} O record from Lisiecki and Raymo, 2005 is displayed on each subplot (black) to show changes in global glaciation. The subplots are enlarged from Fig. 4. Each subplot shows the uncertainty of predicted bulk δ^{234} U (gray envelope, derived from the propagated uncertainty in Eqs. (3) and (4), overlain by observed bulk δ^{234} U. Sections of colored points and bars represent sections where adjacent anomalies of observed bulk δ^{234} U are greater (blue) or less (red) than the uncertainty of predicted bulk δ^{234} U. These four sections were identified by finding values where observed bulk δ^{234} U was significantly higher than the decayed δ^{234} U of seawater and its surrounding intervals of low δ^{234} U.

periods of higher organic rain rate (Fig. 6, green), this relationship is imperfect as the mechanism imparting each may be slightly different and the uncertainty in the age model is generally higher around deglacial terminations.

While we might expect this relationship during these high mass accumulation events, similarities between aU and $\delta^{234}U$ (of lower values) is seen meters into both sides of adjacent sediment. During MIS 5/6, 7/8, and 9/10, $\delta^{234}U$ is high during deglaciation and is relatively low in the periods before and after this peak. MIS 11/12 is similar but has two unique peaks of high $\delta^{234}U$. However, these patterns are not synchronous with the changes in the aU record and are not confined within changes in the benthic $\delta^{18}O$, even given the uncertainty of the age model. Accompanying changes in high or low $\delta^{234}U$ are significantly broader than its aU counterpart, making it appear that the signal is "smeared" over a longer timeframe. Although this "smearing" indicates that any relationship between $\delta^{234}U$ and aU is likely non-linear, correlation between them in only these select intervals suggests a mechanistic link between the two.

3.2. Relationship of $\delta^{234}U$ to pre-alteration model

By finding differences between the predicted bulk $\delta^{234}U$ of the endmember mixing model and the observed δ^{234} U isotope data, we were able to identify sections of ODP 1094 where it is potentially subject to a change in source or post-depositional mobilization of ²³⁴U. We define observed values of δ^{234} U within model expectations, and thereby unaltered, where the uncertainty of observed bulk $\delta^{234}U$ intersects with the uncertainty of predicted bulk δ^{234} U (Fig. 5). In total, 283 of 595 data points (47%) fell outside of model expectations (Fig. 6), which represents a significant fraction of geologic time in the core. Small anomalies were found within glacial-interglacial periods, however the largest deviation from model expectations occurred within adjacent sections surrounding deglacial transitions MIS 5/6, 7/8, 9/10, and 11/12 (Fig. 7). These anomalies were characterized by high δ^{234} U peaks, that were significantly greater than the decayed seawater endmember, which are bordered by sections with low anomalies (red and blue bars on Fig. 7).

4. Discussion

4.1. Constraining potential changes to sedimentary $\delta^{234}U$

Given the results of our model, $\delta^{234} U_{anomaly}$ represents either periods with a change to the isotopic source of U or intervals where ^{234}U is lost/ gained after burial. To investigate the cause for anomaly at ODP 1094, we can look at three general cases that can change the δ^{234} U in pelagic sediments; (1) change in the δ^{234} U of local bottom water, (2) change in U source from particulate material, and (3) rearrangement of U after burial. Some of these cases are discussed in detail later in the discussion, however, we can use observed data to constrain any potential mechanism based on what parameters it would need to explain the observations. In the first case, U and other redox sensitive metals indicate that >70% of U is formed from seawater (Rohde et al., 2021). Changes to local bottom water δ^{234} U affect the isotopic composition precipitated into the aU fraction. Given MIS 9/10 as an example, modern observations would require that the local composition of seawater was roughly double to sixfold that of modern seawater (~300–900%) during positive ²³⁴U_{anomaly} and similar to detrital material during negative ²³⁴U_{anomaly}. This idea is inconsistent with the consensus that the $\delta^{234}U$ of global seawater is relatively unchanged over multiple glacial periods. There are some mechanisms which may change the U isotope chemistry in specific areas, such as pulses of subglacial meltwater, however these mechanisms cannot explain both the positive and negative 234Uanomaly surrounding deglacial terminations.

In the second case, particle sources might act to change the total δ^{234} U of sediments; however, this effect would be dependent on the original particle's U chemistry and its interaction with bottom sediments. For example, particles derived from organic matter generally do not add a large source of U into sediment in an oxygenated water column (Anderson, 1982), but are a catalyst for benthic respiration and redox potential that precipitates U from seawater. We might expect that periods with heavy organic rain bury aU strongly at the isotopic composition of seawater. Similarly, erosion of the sediment and/or transport of older materials to the core site would drive δ^{234} U towards 0‰ as this material is aged towards secular equilibrium (Abshire et al., 2020). If there were a source of other particles with unique U chemistry, such as hydrothermal particles, their isotopic composition must be over an order of magnitude greater than the δ^{234} U of seawater to explain our observations with their low abundance.

Due to these constraints in the first two cases, we believe that case three, diagenetic rearrangement of ^{234}U is the most likely explanation for our observations of $\delta^{234}\text{U}$ at ODP 1094. Diagenetic rearrangement potentially explains the patterns of positive and negative $^{234}\text{U}_{anomaly},$ which may indicate pathways for U mobilization. It also has power in explaining incongruencies in the timing of $^{234}\text{U}_{anomaly}$ features compared to the deglacial transition, as the degree of diagenesis and mass accumulation rate may play a role in the vertical extent of U mobilization.

4.2. Relationship between aU and $\delta^{234}U$

The anomalous patterns observed may be explained by the differences in the reprecipitation potential of alpha-recoiled U in sediments. As we can assume that once aU is precipitated and no process re-oxidizes the sediment, the vast majority of the U remains reduced and immobile. The presence of aU at all depths of this record means there is functionally no U concentration in surrounding pore waters; however, ²³⁴U is introduced into the pore water when alpha-recoil occurs, acting as a relatively constant source of ²³⁴U to all sediment layers over time. Some of this ²³⁴U may reprecipitate back in place, but this effect will be stronger in intervals with greater reducing capacity, such as those with high organic delivery during deglaciation. A mechanism proposed for the reduction of aU is the active respiration of sulfate/Fe reducing bacteria, which may explain why intervals with the highest organic

carbon flux, and thereby the highest sustained respiration, might act as persistent sinks of U (Lovley et al., 1993). Stronger rates of reprecipitation at these intervals drive lower ^{234}U concentration in surrounding pore water compared to adjacent sediment layers. In turn, this gradient in ^{234}U concentration in pore water drives diffusion of ^{234}U towards these highly reducing layers. Given the diffusivity coefficient of U in pore water (3 \times 10 $^{-6}$ cm 2 s $^{-1}$ Klinkhammer and Palmer, 1991) and the age of sediment older that MIS 5, there is theoretically enough time for ^{234}U to diffuse over the vertical distances observed across anomalous sections, although we might expect the actual residence time of U in pore water to be much shorter.

The transport of ²³⁴U in pore water can be generally described by diffusion, advection, and exchange with the sediment interface (Maher et al., 2004). As pore water contains a small proportion of U in the overall sediment-fluid system, U's residence time in reducing waters is relatively short and the isotopic composition of U mainly reflects exchange with the solid phase, rather than vertical transport within the sediment column (Maher et al., 2004). As ODP 1094 experiences constant suboxic conditions, reprecipitation from reducing sediments may be weak enough that ²³⁴U can redistribute vertically to some degree within pore waters. Ignoring vertical advection in the sediment column, the diffusive transport of ²³⁴U in pore water between two sediment depths can be simplified to the following:

$$F_d = \Delta [F_\alpha - F_s] = D^* \frac{\Delta [^{234}U]_{PW}}{\Delta x}$$
(8)

where F_d is the vertical flux of ^{234}U in pore water by diffusion between two depth intervals, F_α is the flux of ^{234}U from sediment into pore water due to alpha-recoil, F_s is the flux of alpha-recoiled ^{234}U precipitation, D is the diffusivity coefficient for U in sediment pore water, $\Delta [^{234}U]_{PW}$ is the difference in ^{234}U concentration between pore water intervals, and Δx is the vertical distance between pore water intervals. These equations are shown as a schematic in Fig. 8.

Pore water redistribution of alpha-recoiled ^{234}U is able to explain some observations that a change in burial source cannot. For example, this explains the relationship of $^{234}\text{U}_{anomaly}$ to sediment age better than burial source, as instead of having extreme changes in the $\delta^{234}\text{U}$ of seawater which cannot be explained with simple lead or lag, diagenesis by rearrangement of ^{234}U in pore water is simply related to the redox

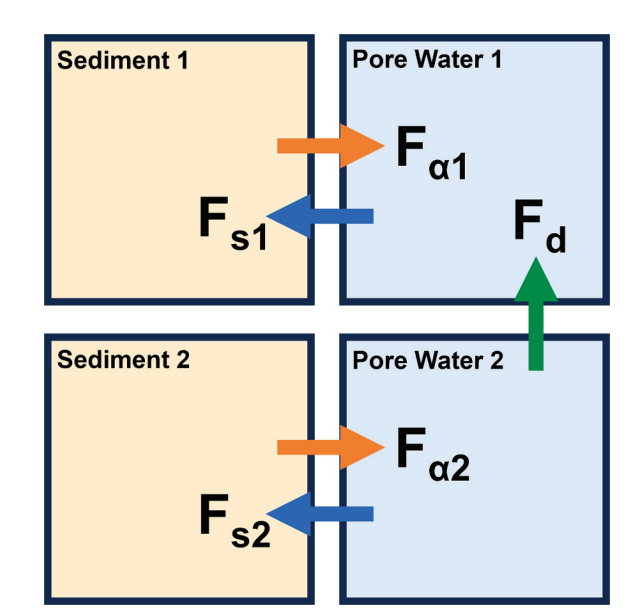


Fig. 8. Schematic for flux of alpha-recoiled ^{234}U between two sediment layers. F_d is the vertical flux of ^{234}U in pore water by diffusion between two depth intervals, F_α is the flux of ^{234}U from sediment into pore water due to alpharecoil, F_s is the flux of alpha-recoiled ^{234}U precipitation.

state of the sediment when buried. Also, since these pore waters are nearly entirely 234 U, and thereby a source δ^{234} U much higher than most other environmental processes. It should be noted that although this mechanism explains the apparent relationship between sediment aU and $\delta^{234}\text{U}$ at ODP 1094 and other open ocean records (such as site 90-13-13 in the Labrador Sea (Vallières, 1997), or the Lomonosov Ridge (Purcell et al., 2022), some types of geologic settings or diagenetic effect can reverse the apparent relationship. For example, in environments where aU is built from periods of intensely reducing conditions, the sediment above and below may have a similar reduction capacity, and when alpha-recoil occurs this weaker contrast might cause the gradient in pore water ²³⁴U to diffuse outward from the peak in aU. ODP 1094 might be different in this regard as changes in aU are relatively within a few ppm of its background, so aU precipitation represents only small changes within suboxic conditions (Rohde et al., 2021). After undergoing burndown, Mediterranean sapropels described by Gourgiotis et al., 2011, Mangini and Dominik, 1979, and Severmann and Thomson, 1998 show ²³⁴U diffused away from peaks of aU built by the re-oxidation front. For sediment that has undergone strong redox changes, the processes controlling the gradient of ²³⁴U in pore water, unlike ODP 1094, may not solely be the result of differences in reprecipitation of alpha-recoiled ²³⁴U.

4.3. Balance of ²³⁴U in anomalous intervals

The results of our mass balance (Table 1) lend support to the hypothesis that anomalies at the four MIS transitions of interest are contributed to by pore water diffusion and rearrangement of preferentially mobilized ²³⁴U near aU peaks. We might expect that in a closed system, where the only change to δ^{234} U was due to internal reorganization, that the difference in ²³⁴U_{anomaly}, between sections with excess ²³⁴U and deficient ²³⁴U, would be roughly zero as U is neither added nor removed from the system. This seems to be roughly the case for MIS 7/8 and MIS 11/12 as their total excess ²³⁴U are marginally small within propagated error. However, this is not the case at MIS 5/6 and MIS 9/10 where a significant amount of additional ²³⁴U is present, and in this case points to there being an additional external source of ²³⁴U. All four anomalous sections have deficiencies of relatively similar scale (~-1 to -4 pg/cm²), which is evidence that all sections undergo a similar change from diffusive loss of ²³⁴U, but the fact that they vary on the scale of excess (~5-50 pg/cm²) evidences that MIS 5/6 and 9/10 require an additional source ²³⁴U not accounted for in our original modeling.

4.4. Sources of additional ²³⁴U during MIS 5/6 and MIS 9/10

We find that a significant portion of δ^{234} U at ODP 1094 can be explained given its initial formation from authigenic and detrital sources, particularly during glacial and interglacial sections. From the

Table 1 A mass balance was performed by integrating observed bulk $\delta^{234}U$ and predicted bulk $\delta^{234}U$ with depth (Fig. 4, Fig. 8) into a ^{234}U inventory. Uncertainty of mass integration is reported as the propagation of error from the uncertainty of $\delta^{234}U$ measurement at 2σ . Anomaly Section – Time period of interest. Depth – depth range of interest. Def ^{234}U – Combined integrated mass of ^{234}U below model prediction from both negative $^{234}U_{anomaly}$ sections surrounding deglacial terminations. Ex ^{234}U – Integrated mass of ^{234}U above model prediction at positive anomaly features. Net ^{234}U – Net excess ^{234}U – Ex ^{234}U - Def ^{234}U .

Anomaly Section	Depth(m)	Def ²³⁴ U(pg/ cm ²)	Ex ²³⁴ U(pg/ cm ²)	Net ²³⁴ U(pg/ cm ²)
MIS 5/6 MIS 7/8 MIS 9/10 MIS 11/12 Full Record to 504 ka	21–27 34–44 49–54.5 56–73 0.57–75.14	-3.8 ± 0.5 -1.5 ± 0.4 -3.8 ± 0.7 -3.3 ± 0.7 -13.9 ± 1.5	25.4 ± 1.6 4.7 ± 0.9 16.5 ± 1.5 4.8 ± 0.9 52.9 ± 2.6	21.6 ± 1.7 3.2 ± 1.0 12.7 ± 1.7 1.5 ± 1.1 39.1 ± 2.9

anomalies that occur during deglacial transition, the entire anomaly from MIS 7/8 and 11/12, and part of the anomaly from MIS 5/6 and 9/10, can be explained by diffusion of alpha-recoiled $^{234}\mathrm{U}$. However, the mass balance of MIS 5/6 and 9/10 shows that $\delta^{234}\mathrm{U}$ anomalies cannot be fully explained by a simple rearrangement of existing $^{234}\mathrm{U}$. While a total explanation for this phenomenon is elusive, we look to evaluate some candidate sources to narrow potential processes. The constraints of these potential processes are the same as mentioned earlier in the discussion.

One candidate explanation is the same diffusive transport of alpharecoiled ²³⁴U mechanism is also happens laterally across depth horizons. Variation in the sediment accumulation rate, and thereby aU accumulation, is seen across cores in the Atlantic sector of the Southern Ocean (Frank et al., 2000). With this variation in burial we might expect that, at a certain spatial scale, strong redox features might be vertically offset. The redox state of pore water at any given depth will vary laterally, which in turn might create gradients of pore water 234U, driving local transport. Given the diffusivity coefficient of U in pore water, U can travel a little over 300 km per hundred thousand years, and although we might expect ²³⁴U residence time in pore water to be shorter, this potentially allows ²³⁴U to pool at relatively higher ²³⁴U_{anomaly} from surrounding sediment. The observed ²³⁴U_{anomaly} excess seen in MIS 5/6 and 9/10, could imply that these layers have a higher reduction capacity than other sediment at this depth horizon and that other cores might have corresponding negative anomalies elsewhere in the region. This mechanism also has some power in explaining small $^{234}\mbox{U}_{anomaly}$ that were seen outside of deglacial termination, as some localized diffusion might occur based on differing redox conditions with surrounding sediment. Future work will need to look at U in sediment and pore waters within this ocean region to determine if geographic difference in pore water redox state can drive changes to ²³⁴U in the way we have observed.

Another candidate explanation for this unaccounted source of ²³⁴U includes the flux of ²³⁴U enriched Antarctic meltwater. This mechanism involves subglacial weathered ²³⁴U becoming entrained in glacial meltwater and over time significantly enriching the water with highly positive δ^{234} U, being released as its reservoirs melt. Glacial meltwater can potentially impact U forming sediments in two ways; (1) as a pulse of freshwater to nearby shelf systems, or (2) as changes to global seawater as these meltwaters pulses integrate with it over time. Considering the first case, it has been observed that parts of the Greenland Ice Sheet (Arendt et al., 2018) and the Wilkes Basin (Blackburn et al., 2020) exhibit δ^{234} U more positive than our observed data, showing that subglacial water signals are potentially strong enough to explain our data. The issue with this mechanism is that there is no direct pathway for fresh Antarctic meltwater source to permeate in Antarctic Bottom Water to the degree needed to match observations. In the second case, these pulses can become integrated into the global $\delta^{234} \text{U}$ over glacial-interglacial time scales (Esat and Yokoyama, 2006; Robinson et al., 2004), potentially leading to a variable isotopic composition in seawater between 120 and 180% (Arendt et al., 2018). This change to global seawater due to subglacial meltwater has been invoked to explain the evolution of δ^{234} U in paleo coral records (Chen et al., 2016; Esat and Yokoyama, 2006). The change in the δ^{234} U of seawater in these records is on the scale of 10's of ‰, which is ultimately smaller than is needed to explain the positive $\delta^{234}U$ anomalies at ODP 1094.

A mechanism that may similarly affect globally integrated δ^{234} U of seawater is from the re-dissolution of coastal sediments during sea level rise. During interglacials and interstadials, there is an increased number of environments, such as margins, slopes, marshes, and mangroves, which are overlain by oxygen depleted water, which build U and excess 234 U concentrations (Chen et al., 2016; Dunk et al., 2002; Esat and Yokoyama, 2006). These sediments are oxidized during low stands and return to the ocean as sea level rises. If this process were to have a major effect on deep ocean sediment, we might also expect it to have a large effect on the more proximal coral records, in which we would expect increases matching the same magnitude of ODP 1094. This does not

seem to be the case, however, as studies like that of Chen et al. (2016), show much smaller variation (<10%) in δ^{234} U which is asynchronous with sea level rise.

The final candidate explanation involves ferromanganese deposits enriched via the leaching of low temperature hydrothermal fluid or volcanics (Herbert Veeh and Boström, 1971; MacDougall et al., 1979). Global hydrothermal activity is hypothesized to increase during glacial terminations (Lund et al., 2016). Changes in ice sheet dynamics drive sea-level weighted pressure change on the upper mantle, which ultimately modulate melt production and by extension, hydrothermal activity (Huybers and Langmuir, 2009; Lund et al., 2016; Lund and Asimow, 2011). Ferromanganese deposits have variable $\delta^{234}U$ which is often within 20% of seawater, but has been observed to be as high as twice that of seawater (Reyss et al., 1987). While this means that hydrothermal particles are potentially enriched to the same degree as our high observations, this would require a larger percent of the U in ODP 1094 to be hydrothermal than is possible. For example, from the observed δ^{234} U of hydrothermal particles given by Reyss et al., 1987, ODP 1094 would require nearly 100% of the sediment U to be a hydrothermal ferromanganese fraction. This cannot be the case as clean mineral analysis of TN057-13PC4, a piston core from the same location covering the last deglacial period, show quartz chemistry that is not characteristic of hydrothermal origin (Nielsen and Hodell, 2007). While it is possible that volcaniclastics play a small role in $\delta^{234}\text{U}$ changes in deep sea sediment, a lack of observed hydrothermal proxies make this scenario unlikely to account for ODP 1094's δ^{234} U anomalies.

4.5. Broader impact

Analysis of sedimentary $\delta^{234}U$ at ODP 1094 has shown that $\delta^{234}U$ is a useful proxy in the pelagic ocean that can capture processes that are not identified by the bulk U concentration. On a broad scale, this is important for understanding the marine cycling of U, and its use as a paleoceanographic proxy. In some environmental settings, the diagenesis of solely ²³⁴U might be enough to impact paleoredox interpretations and would be hard to observe given only the bulk concentration. Outside of its context in informing bulk U cycling, δ^{234} U is potentially useful in tracing sediment-pore water interactions after burial. As the pool of alpha-recoiled ²³⁴U in pore water is sensitive to both the redox state of the sediment it was originally buried in and to suboxic changes in pore water redox, it has a unique role amongst redox sensitive trace metals tracking both. For example, in an environment where sediment has undergone a small amount of redox remobilization, or burn-down, the δ²³⁴U should have a unique pattern of diagenetic alteration from this effect. In theory, this concept can be applied to all other redox sensitive trace metals that alpha decay as they will go through the same process, but to differing degrees based on environmental condition.

5. Conclusions

The U isotopic composition of ODP 1094 shows a relationship with sedimentary aU during deglacial periods of high organic rain and in surrounding sediment, but not throughout the entire record. Observed bulk δ^{234} U was compared to a model predicting δ^{234} U where distinct pattern sections of alternating positive and negative anomalies potentially evidenced post-depositional diagenesis during these features. Our results show a significant amount of δ^{234} U observations at ODP 1094 are explained by its initial formation given authigenic and detrital components. Major sections of anomaly, identified by periods where $\delta^{234} U$ was greater than seawater $\delta^{234}U$ and its surrounding sediment of negative anomaly, were observed at MIS 5/6, 7/8, 9/10, and 11/12. It was observed that deglacial intervals with increased organic rain and increased reducing capacity act as a sink for ²³⁴U that is alpha-recoiled and diffused from surrounding sediment. This remobilization of ²³⁴U towards peaks of aU explains anomalies at MIS 7/8 and 11/12 entirely, and partially at MIS 5/6 and 9/10. This is evidence to support the use of δ^{234} U to identify diagenetic features in other similar pelagic sediments, however we find that deviations in δ^{234} U from expectations do not only reflect vertical diagenetic changes. An additional source of enriched δ^{234} U, present during some deglacial transitions, may be needed to explain the remaining excess 234 U during MIS 5/6 and MIS 9/10. Given the constraints that potential sources would need to fulfil to meet the observations at ODP 1094, the most likely scenario is that diagenesis is responsible for this. Excess 234 U is potentially explained by diffusion of alpha-recoiled 234 U across sediment depth horizon, however, further study is warranted to address this conclusion. The implications of this phenomenon may be important in understanding deep sea redox state and its controls on the sedimentary U budget.

Declaration of Competing Interest

The authors declare that they have no known competing financial interests or personal relationships that could have appeared to influence the work reported in this paper.

Data Availability

Data is available at Zenodo.org at https://doi.org/10.5281/zenodo. 6959606.

Acknowledgements

This work was funded by the US National Science Foundation (award 1658445). ODP samples used here were provided by the Bremen Core Repository. Additional thanks to current and past members from the labs of Dr. Christopher Hayes and Dr. Alan Shiller at the University of Southern Mississippi, for help with sample preparation and facility use, especially Melissa Gilbert for expertise with the ICP-MS.

References

- Abshire, M.L., Romaniello, S.J., Kuzminov, A.M., Cofrancesco, J., Severmann, S., Riedinger, N., 2020. Uranium isotopes as a proxy for primary depositional redox conditions in organic-rich marine systems. Earth Planet. Sci. Lett. 529.
- Andersen, M.B., Stirling, C.H., Zimmermann, B., Halliday, A.N., 2010. Precise determination of the open ocean ²³⁴U/²³⁸U composition. Geochem. Geophy. Geosy. 11 (12).
- Andersen, M.B., Vance, D., Morford, J.L., Bura-Nakić, E., 2016. Closing in on the marine ²³⁸U/²³⁵U budget. Chem. Geol. 420, 11–22.
- Andersen, M.B., Stirling, C.H., Weyer, S., 2017. Uranium isotope fractionation. Non-Traditional Stable Isotopes. 82, 799–850.
- Anderson, R.F., 1982. Concentration, vertical flux, and remineralization of particulate uranium in seawater. Geochim. Cosmochem. Ac. 46, 1293–1299.
- Anderson, R.F., Sachs, J.P., Fleisher, M.Q., Allen, K.A., Yu, J., Koutavas, A., Jaccard, S.L., 2019. Deep-sea oxygen depletion and ocean carbon sequestration during the last ice age. Global Biogeochem. Cy. 33 (3), 301–317.
- Arendt, C.A., Aciego, S.M., Sims, K.W.W., Das, S.B., Sheik, C., Stevenson, E.I., 2018.
 Influence of glacial meltwater on global seawater δ²³⁴U. Geochim. Cosmochim. Ac. 225, 102–115.
- Blackburn, T., Edwards, G.H., Tulaczyk, S., Scudder, M., Piccione, G., Hallet, B., Mclean, N., Zachos, J.C., Cheney, B., Babbe, J.T., 2020. Ice retreat in Wilkes Basin of East Antarctica during a warm interglacial. Nature 583.
- Bourne, M.D., Thomas, A.L., Niocaill, C.M., Henderson, G.M., 2012. Improved determination of marine sedimentation rates using 230 Th_{xs}. Geochem. Geophy. Geosy. 13 (1), 1–9.
- Brewer, P.G., Nozaki, Y., Spencer, D.W., Fleer, A.P., 1980. Sediment trap experiments in the deep north Atlantic: isotopic and elemental fluxes. J. Mar. Res. 38 (4), 703–728. Broecker, W.S., 1982. Ocean chemistry during glacial time. Geochim. Cosmochim. Ac. 46 (10), 1689–1705.
- Chen, T., Robinson, L.F., Beasley, M.P., Claxton, L.M., Andersen, M.B., Gregoire, L.J., Wadham, J., Fornari, D.J., Harpp, K.S., 2016. Ocean mixing and ice-sheet control of seawater ²³⁴U/²³⁸U during the last deglaciation. Science 354 (6312), 626–629.
- Cheng, H., Lawrence Edwards, R., Shen, C.C., Polyak, V.J., Asmerom, Y., Woodhead, J., Hellstrom, J., Wang, Y., Kong, X., Spötl, C., Wang, X., Calvin Alexander, E., 2013. Improvements in ²³⁰Th dating, ²³⁰Th and ²³⁴U half-life values, and U-Th isotopic measurements by multi-collector inductively coupled plasma mass spectrometry. Earth Planet. Sci. Lett. 371–372, 82–91.
- Chutcharavan, P.M., Dutton, A., Ellwood, M.J., 2018. Seawater ²³⁴U/²³⁸U recorded by modern and fossil corals. Geochim. Cosmochim. Ac. 224, 1–17.
- Delmas, R.J., Ascencio, J., Legrand, M., 1980. Polar ice evidence that atmospheric CO_2 20,000 yr BP was 50% of present. Nature 284, 155–157.

Nature 389, 929-935.

- DePaolo, D.J., Maher, K., Christensen, J.N., McManus, J., 2006. Sediment transport time measured with U-series isotopes: Results from ODP North Atlantic drift site 984. Earth Planet. Sci. Lett. 248 (1–2), 394–410.
- DePaolo, D.J., Lee, V.E., Christensen, J.N., Maher, K., 2012. Uranium comminution ages: Sediment transport and deposition time scales. C. R. Geosci. 344 (11–12), 678–687.
- Dunk, R.M., Mills, R.A., Jenkins, W.J., 2002. A reevaluation of the oceanic uranium budget for the Holocene. Chem. Geol. 190 (1–4), 45–67.
- Esat, T.M., Yokoyama, Y., 2006. Variability in the uranium isotopic composition of the oceans over glacial-interglacial timescales. Geochim. Cosmochim. Ac. 70 (16), 4140–4150.
- Firestone, R.B., Baglin, C.M., Chu, F.S.Y., 1998. Table of Isotopes, 8th ed. Wiley. Francois, R., Altabet, M., Yu, E., Sigman, D., Bacon, M., Frank, M., Bohrmann, G., Bareille, G., Layeyrie, L., 1997. Contribution of Southern Ocean surface-water stratification to low atmospheric CO2 concentrations during the last glacial period.
- Francois, R., Bacon, M.P., Altabet, M.A., Labeyrie, L.D., 1993. Glacial/interglacial changes in sediment rain rate in the SW Indian Sector of subantarctic Waters as recorded by $^{230}\text{Th},\,^{231}\text{Pa},\,\text{U},\,\text{and}\,\,\delta^{15}\text{N}.$ Paleoceanography 8 (5), 611–629.
- Frank, M., Gersonde, R., Rutgers van der Loeff, M., Bohrmann, G., Nürnberg, C.G., Kubik, P.W., Suter, M., Mangini, A., 2000. Similar glacial and interglacial export bioproductivity in the Atlantic sector of the Southern Ocean: Multiproxy evidence and implication for glacial atmospheric CO₂. Paleoceanography 15 (6), 642–658.
- Glasscock, S.K., Hayes, C.T., Redmond, N., Rohde, E., 2020. Changes in antarctic bottom water formation during interglacial periods. Paleoceanogr. Paleoclimatol. 35 (8), 1–13.
- Gourgiotis, A., Reyss, J.L., Frank, N., Guihou, A., Anagnostou, C., 2011. Uranium and radium diffusion in organic-rich sediments (sapropels). Geochem. Geophy. Geosy. 12 (9)
- Hasenfratz, A.P., Jaccard, S.L., Martínez-García, A., Sigman, D.M., Hodell, D.A., Vance, D., Bernasconi, S.M., Kleiven, H.F., Haumann, F.A., Haug, G.H., 2019. The residence time of Southern Ocean surface waters and the 100,000-year ice age cycle. Science 363 (6431), 1080–1084.
- Hayes, C.T., Anderson, R.F., Fleisher, M.Q., Serno, S., Winckler, G., Gersonde, R., 2013. Quantifying lithogenic inputs to the North Pacific Ocean using the long-lived thorium isotopes. Earth Planet. Sci. Lett. 383, 16–25.
- Hayes, C.T., Martínez-García, A., Hasenfratz, A.P., Jaccard, S.L., Hodell, D.A., Sigman, D. M., Haug, G.H., Anderson, R.F., 2014. A stagnation event in the deep south Atlantic during the last interglacial period. Science 346 (6216), 1514–1517.
- Hayes, C.T., McGee, D., Mukhopadhyay, S., Boyle, E.A., Maloof, A.C., 2017. Helium and thorium isotope constraints on African dust transport to the Bahamas over recent millennia. Earth Planet. Sci. Lett. 457, 385–394.
- millennia. Earth Planet. Sci. Lett. 457, 385–394.

 Henderson, G.M., 2002. Seawater (²³⁴U/²³⁸U) during the last 800 thousand years. Earth Planet. Sci. Lett. 199 (1–2), 97–110.
- Henderson, G.M., Anderson, R.F., 2003. The U-series toolbox for paleoceanography. Rev. Mineral. Geochem. 52. 493–531.
- Herbert Veeh, H., Boström, K., 1971. Anomalous ²³⁴U/²³⁸U on the East Pacific rise. Earth Planet. Sci. Lett. 10 (3), 372–374.
- Huybers, P., Langmuir, C., 2009. Feedback between deglaciation, volcanism, and atmospheric CO₂. Earth Planet. Sci. Lett. 286 (3–4), 479–491.
- Jaccard, S.L., Hayes, C.T., Martínez-García, A., Hodell, D.A., Anderson, R.F., Sigman, D. M., Haug, G.H., 2013. Two modes of change in Southern Ocean productivity over the past million years. Science 339 (6126), 1419–1423.
- Jaccard, S.L., Galbraith, E.D., Martínez-Garciá, A., Anderson, R.F., 2016. Covariation of deep Southern Ocean oxygenation and atmospheric CO₂ through the last ice age. Nature 530 (7589), 207–210.
- Jaffey, A.H., Flynn, K.F., Glendenin, L.E., Bentley, W.C., Essling, A.M., 1971. Precision measurement of half-lives and specific activities of U²³⁵ and U²³⁸. Phys. Rev. C 4 (5), 1889–1906
- Kanfoush, S.L., Hodell, D.A., Charles, C.D., Janecek, T.R., Rack, F.R., 2002. Comparison of ice-rafted debris and physical properties in ODP Site 1094 (South Atlantic) with the Vostok ice core over the last four climatic cycles. Palaeogeogr. Palaeoclimatol. Palaeoecol. 182 (3–4), 329–349.
- Klinkhammer, G.P., Palmer, M.R., 1991. Uranium in the oceans: Where it goes and why. Geochim Cosmochim Ac. 55 (7), 1799–1806.
- Knight, G.B., Macklin, R.L., 1948. Half-life of U X1(Th234). Phys. Rev. 74, 1540–1541.
 Ku, T., 1965. An evaluation of the U²³⁴/U²³⁸ method as a tool for dating pelagic sediments. J. Geophys. Res. 70 (14).

- Ku, T., Knauss, K., Mathieu, G., 1997. Uranium in open ocean: concentration and isotopic composition. Deep-Sea Res. 24, 1005–1017.
- Lisiecki, L.E., Raymo, M.E., 2005. A Pliocene-Pleistocene stack of 57 globally distributed benthic δ^{18} O records. Paleoceanography 20 (1), 1–17.
- Lovley, D.R., Roden, E.E., Phillips, E.J.P., Woodward, J.C., 1993. Enzymatic iron and uranium reduction by sulfate-reducing bacteria. Mar. Geol. 113 (1–2), 41–53.
- Lund, D.C., Asimow, P.D., 2011. Does sea level influence mid-ocean ridge magmatism on Milankovitch timescales? Geochem. Geophy. Geosy. 12 (12), 1–26.
- Lund, D.C., Asimow, P.D., Farley, K.A., Rooney, T.O., Seeley, E., Jackson, E.W., Durham, Z.M., 2016. Enhanced east pacific rise hydrothermal activity during the last two glacial terminations. Science 351 (6272), 478–482.
- MacDougall, J.D., Finkel, R.C., Carlson, J., Krishnaswami, S., 1979. Isotopic evidence for uranium exchange during low-temperature alteration of oceanic basalt. Earth Planet. Sci. Lett. 42 (1), 27–34.
- Maher, K., DePaolo, D.J., Lin, J.C.F., 2004. Rates of silicate dissolution in deep-sea sediment: In situ measurement using ²³⁴U/²³⁸U of pore fluids. Geochim. Cosmochim. Ac. 68 (22), 4629–4648.
- Mangini, A., Dominik, J., 1979. Late Quaternary sapropel on the Mediterranean Ridge: U-budget and evidence for low sedimentation rates. Sed. Geol. 23 (1–4), 113–125.
- Martin, A.N., Dosseto, A., Kinsley, L.P.J., 2015. Evaluating the removal of non-detrital matter from soils and sediment using uranium isotopes. Chem. Geol. 396, 124–133.
- Nielsen, S.H.H., Hodell, D.A., Kamenov, G., Guilderson, T., Perfit, M.R., 2007. Origin and significance of ice-rafted detritus in the Atlantic sector of the Southern Ocean. Geochem. Geophy. Geosy. 8 (12).
- Nielsen, S.H.H., Hodell, D.A., 2007. Antarctic ice-rafted detritus (IRD) in the South Atlantic; indicators of iceshelf dynamics or ocean surface conditions? Open-File Report U. S. Geolog. Survey. 4 (1999).
- Orsi, A.H., Whitworth, T., Nowlin, W.D., 1995. On the meridional extent and fronts of the Antarctic Circumpolar Current. Deep-Sea Res. 42 (5), 641–673.
- Purcell, K., Hillaire-marcel, C., Vernal, A.D., Ghaleb, B., Stein, R., 2022. Potential and limitation of 230 Th-excess as a chronostratigraphic tool for late Quaternary Arctic Ocean sediment studies: An example from the Southern Lomonosov Ridge. Marine Geol. 448
- Reyss, J.L., Lamitre, N., Bonte, P., Franck, D., 1987. Anomalous ²³⁴U/²³⁸U ratios in deep-sea hydrothermal deposits. Nature 325, 798–800.
- Robinson, L.F., Belshaw, N.S., Henderson, G.M., 2004. U and Th concentrations and isotope ratios in modern carbonates and waters from the Bahamas. Geochim. Cosmochim. Ac. 68 (8), 1777–1789.
- Rohde, E.E., Hayes, C.T., Redmond, N., Glasscock, S.K., 2021. Southern ocean oxygenation changes inferred from redox-sensitive trace metals across marine isotope stage 11. Geochem. Geophy. Geosy. 22 (8), 1–13.
- Romaniello, S.J., Herrmann, A.D., Anbar, A.D., 2013. Uranium concentrations and ²³⁸U/²³⁵U isotope ratios in modern carbonates from the Bahamas: Assessing a novel paleoredox proxy. Chem. Geol. 362, 305–316.
- Severmann, S., Thomson, J., 1998. Investigation of the ingrowth of radioactive daughters of ²³⁸U in Mediterranean sapropels as a potential dating tool. Chem. Geol. 150 (3–4), 317–330.
- Shipboard Scientific Party. 1999a. Leg 177 summary. Paleoceanography, 177.Shipboard Scientific Party. 1999b. Site 1094. Proceedings of the Ocean Drilling Program,Initial Reports, 177.
- Sigman, D.M., Hain, M.P., Haug, G.H., 2010. The polar ocean and glacial cycles in atmospheric CO₂ concentration. Nature 466 (7302), 47–55.
- Thomas, A.L., Henderson, G.M., McCave, I.N., 2007. Constant bottom water flow into the Indian Ocean for the past 140 ka indicated by sediment 231 Pa/ 230 Th ratios. Paleoceanography 22 (4).
- Vallières, S., 1997. Flux d'uranium au cours des processus diagénétiques. L' Université du Ouébec à Montréal. 2.
- Villa, I.M., Bonardi, M.L., De Bièvre, P., Holden, N.E., Renne, P.R., 2016. IUPAC-IUGS status report on the half-lives of 238 U, 235 U and 234 U. Geochim. Cosmochim. Ac. 172, 387–392.
- Wilson, T.R.S., Thomson, J., Hydes, D.J., Colley, S., Culkin, F., Sørensen, J., 1986.
 Oxidation fronts in pelagic sediments: Diagenetic formation of metal-rich layers.
 Science 232, 972–975.
- Yokoyama, Y., Esat, M., Lambeck, K., 2001. Coupled climate and sea-level changes deduced from Huon Peninsula coral terraces of the last ice age. Earth Planet. Sci. Lett. 193, 578–587.
- Zhou, Y., McManus, J., 2022. Extensive evidence for a last interglacial Laurentide outburst (LILO) event. Geology 50.